

Experimental super-resolved phase measurements with shot-noise sensitivity

L. Cohen, D. Istrati, L. Dovrat, and H. S. Eisenberg

Racah Institute of Physics, Hebrew University of Jerusalem, Jerusalem 91904, Israel

The ultimate sensitivity of optical measurements is a key element of many recent works. Classically, it is mainly limited by the shot noise limit. However, a measurement setup that incorporates quantum mechanical principles can surpass the shot noise limit and reach the Heisenberg limit. Nevertheless, many of those experiments fail to break even the classical shot-noise limit. Following a recent proposal, we present here the results of optical phase measurements with a photon-number resolving detector using coherent states of up to 4200 photons on average. An additional scheme that can be implemented using standard single-photon detectors is also presented, and the results of the two schemes are compared. These measurements present deterministic single-shot sub-wavelength super-resolution up to 288 better than the optical wavelength. The results follow the classically limited sensitivity, up to 86 times better than the wavelength.

PACS numbers: 06.20.Dk, 42.25.Hz, 42.50.Ar

One of the most common ways to sense and measure the physical world is by using electromagnetic radiation, and in particular light. Usually, the sensitivity of such measurements is governed by the quality of the measuring device, but ultimately, this sensitivity is bounded by fundamental physical limits on the measurement uncertainty [1]. The resolution of a measurement, defined as the width of its smallest detail, follows in most cases the scale of the light's wavelength (λ). Nevertheless, the sensitivity scale is not the resolution. Instead, it is determined by the measurement signal-to-noise ratio and can exceed the resolution by many orders of magnitude. For classical measurement devices, sensitivity is limited by the shot noise limit (SNL) – the discrete division of light energy into photons and their Poissonian statistics.

Interestingly, both resolution and sensitivity can be further enhanced. Super-resolved phase measurements, where the smallest detail is smaller than the Rayleigh limit ($\lambda/2$), have been demonstrated with many approaches, using either classical or quantum light sources. The shot noise limit is surpassed by super-sensitive methods that incorporate nonclassical states of light and measurements. As states with non-Poissonian statistics can be used, sensitivity is only limited by the Heisenberg uncertainty principle [2]. Most notable is the use of squeezed states for this purpose [3]. In the last decade there has also been a wide interest in the so-called NOON states [4], as they exhibit both super-resolution and super-sensitivity. These states are superpositions of N photons in one mode and none in the other, and the opposite arrangement of no photons in the first and N in the second.

By using NOON states, super resolution has been demonstrated for states with $N = 2$ [5], $N = 3$ [6], $N = 4$ [7], and $N = 5$ [8]. Nevertheless, sensitivity has only been improved up to 1.59 times better than the SNL, in a probabilistic manner where the signal is post-selected from a larger set of outcomes [7]. Using hyper-entanglement be-

tween ten degrees of freedom of five photons, 10 times resolution enhancement has been demonstrated, as well as 13% sensitivity enhancement for four photons with eight degrees of freedom [9]. Regrettably, despite their advantages, NOON states are hard to generate, vulnerable to noise, and require special detection setups.

Unlike NOON states, optical coherent states are generated by common lasers. They are reduced by absorption to weaker coherent states, thus keeping their qualitative behavior. Enhanced resolution can be achieved by using the photons simultaneously in a few parallel measurements [10], or consecutively by recycling them through a series of measurements [11, 12]. The Fabry-Pérot interferometer is a standard example for the latter. Alternatively, the measuring apparatus can measure properties other than just the average power. Such enhancement has been demonstrated by post-selecting the projection of the output of an interferometer onto a Fock state of 7 photons [13], and onto a NOON state of $N = 6$ [14], and deterministically by homodyne detection [15].

In this Letter we present the experimental results of a recently proposed scheme by Gao *et al.*, that enables the demonstration of super-resolution, while staying at the SNL [16]. It combines standard interferometry of coherent states with a special nonclassical measurement that requires photon-number resolving detectors. Additionally, we show how a similar scheme, that uses only single-photon detectors that cannot resolve the number of photons, achieves super-resolution which is only marginally worse than the original proposal, while keeping the same shot noise limited sensitivity.

The special measurement we applied in this work is the photon-number parity. The parity operator is defined as $\hat{\pi} = (-1)^{\hat{N}}$, where \hat{N} is the photon number operator. Its expectation value is $\langle \hat{\pi} \rangle = \sum_{n=0}^{\infty} (-1)^n P_n$, where P_n is the probability for n photons in the detected state. The parity expectation value reflects the oddness or evenness of the photon number distribution. For example, the par-

ity of a Fock state is 1 or -1 for an even or odd N , respectively. Parity measurements were first used with trapped ions [17], and later in the context of optical interferometry [18, 19]. Apparently, parity measurements are advantageous for many light sources [20, 21] and can even break the Heisenberg limit if the light source is a two mode squeezed vacuum state [22]. It can be detected indirectly using homodyne techniques [15, 23], or directly by observing the photon-number distribution with a photon-number resolving detector, as demonstrated here.

Consider a Mach-Zehnder interferometer whose input is a coherent state from one port and the vacuum from the other. The relative phase ϕ between its arms is the variable we would like to measure, while we observe the state of one of the two output ports. The detected output state is a phase sensitive coherent state $|\alpha(\phi)\rangle$. The parity expectation value of this state is [16]

$$\langle\alpha|\hat{\pi}|\alpha\rangle = e^{-2|\alpha|^2} = e^{-2\bar{n}\cos^2(\frac{\phi}{2})} \xrightarrow{\phi \rightarrow \pi} e^{-\frac{\bar{n}(\phi-\pi)^2}{2}}, \quad (1)$$

where $\bar{n} = |\alpha(0)|^2$ is the maximal detected average photon number, which already includes the effects of photon loss in the interferometer and in the detector. This expectation value is approaching zero as the average number of output photons and its distribution width are increased, because wider distributions include odd and even terms more evenly. On the other hand, when the average photon number is approaching zero, the parity approaches one, as the dominant term becomes P_0 , an even term. When the resolution is defined as half width at $1/e$ of the maximum, the parity measurement resolution is $\sqrt{2/\bar{n}}$. The parity measurement sensitivity saturates the SNL [16, 22]. It is derived using quantum estimation theory to be

$$\Delta\phi = \frac{\Delta\hat{\pi}}{|\frac{d\langle\hat{\pi}\rangle}{d\phi}|} \xrightarrow{\phi \rightarrow \pi} \frac{1}{\sqrt{\bar{n}}} \left(1 + (2\bar{n} + 1) \frac{(\phi - \pi)^2}{8}\right), \quad (2)$$

where the parity uncertainty is $\Delta\hat{\pi} = \sqrt{1 - \langle\hat{\pi}\rangle^2}$ [13].

The major contribution that the P_0 component has on parity at its peak suggests that this value is responsible for most of the improvement in resolution and sensitivity. We explore this option as P_0 can also be obtained by a standard single-photon detector that cannot discriminate between different photon numbers. Its two outcomes, no photon and any number of photons, corresponds to the measurement of P_0 and $P_r = \sum_{n=1}^{\infty} P_n$, respectively. One may assume that the difference between these two values is a better approximation of parity, as the deviation is only at the third term P_2 . Nevertheless, as $P_0 - P_r = 2P_0 - 1$, considering only P_0 is equivalent, and much simpler to evaluate.

The observable for no detection is the zero photon projector $\hat{Z} = |0\rangle\langle 0|$, and its expectation value P_0 is

$$\langle\alpha|\hat{Z}|\alpha\rangle = e^{-|\alpha|^2} = e^{-\bar{n}\cos^2(\frac{\phi}{2})} \xrightarrow{\phi \rightarrow \pi} e^{-\frac{\bar{n}(\phi-\pi)^2}{4}}. \quad (3)$$

This is a very similar result to Eq. 1, with a super-resolved peak which is only wider by $\sqrt{2}$. In order to find the sensitivity of this measurement, we follow the same procedure as in Eq. 2 and obtain

$$\Delta\phi = \frac{\Delta\hat{Z}}{|\frac{d\langle\hat{Z}\rangle}{d\phi}|} \xrightarrow{\phi \rightarrow \pi} \frac{1}{\sqrt{\bar{n}}} \left(1 + \left(\frac{\bar{n}}{2} + 1\right) \frac{(\phi - \pi)^2}{8}\right), \quad (4)$$

where we used $\Delta\hat{Z} = \sqrt{P_0(1 - P_0)}$. Surprisingly, the P_0 measurement is also shot-noise limited.

In order to realize the measurements discussed above, we use a polarization version of the Mach-Zehnder interferometer, where the two spatial modes are replaced by the horizontal and vertical polarizations. In order to achieve better visibility, the polarization modes are not coupled by $\lambda/2$ wave-plates. Instead, the input and output photons pass through Glan-Thompson polarizers oriented at 45° . The relative phase between the polarization modes is introduced by tilting a calibrated 2 mm thick birefringent calcite crystal. An identical crystal oriented at 90° is used to compensate for temporal walk-off. The output is directed to a silicon photo-multiplier (SiPM) detector, which is an array of many single-photon detecting elements, and thus has photon-number sensitivity. The input state is generated by a Ti:Sapphire laser with 780 nm wavelength, that produces 150 fs long pulses. The pulses are picked to reduce their rate to 250 kHz. The average number of photons per pulse is controlled by calibrated neutral density filters.

There are a few effects that distort the original photon statistics as registered by SiPM detectors [24, 25]. The imperfect detection efficiency reduces the average detected photon number, but does not affect its Poissonian

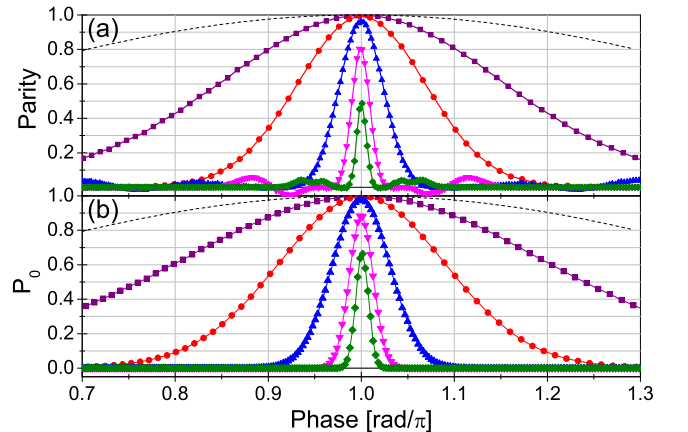


FIG. 1. (color online) Parity (a) and P_0 (b) dependence on the phase difference between the two polarization modes. The presented measurements are for average photon numbers of 4.6 ± 0.2 (purple squares), 25 ± 1 (red circles), 200 ± 8 (blue triangles), 1190 ± 50 (pink inverted triangles), and 4150 ± 150 (green rhombuses). The dashed black lines represent the classic interference curves, for comparison reasons. Errors are not shown, as they are smaller than the symbols.

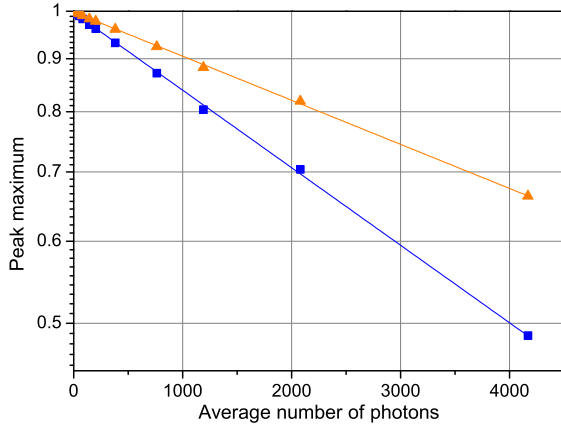


FIG. 2. (color online) The effects of finite visibility and dark counts on the signal peak heights for parity (blue squares) and P_0 (orange triangles). The peak heights are decreased when states with more photons are used, according to Eq. 5.

statistics. Dark counts are false detections as a result of thermal excitations. Cross-talk can trigger neighboring elements of photon triggered elements, and thus falsely increase the number of detected photons. Finally, there is a chance for more than one photon to hit the same detecting element as a result of their finite number (100 in our case). As around the significant region of our measurement $|\alpha| \ll 1$, only dark counts affect it, and their effect is important only for relatively small \bar{n} .

Figure 1 presents the super-resolved signals obtained for parity (Fig. 1a) and P_0 (Fig. 1b). The data sets are for increasing average photon numbers. A clear narrowing of the signals is observed, where the narrowest peak was measured for parity with about 4000 photons. This peak's width is $\lambda/(288 \pm 3)$, corresponding to resolution which is 144 times better than what is regularly achieved (presented for comparison by a black dashed line). The corresponding widths of the curves for parity and P_0 differ by $\sqrt{2}$, as expected from theory. Another difference between the two results is the weak oscillations that appear only for parity. They are a result of the truncation of the parity measurement at 26 photons, which becomes more significant as more photons are involved.

The degradation of the peak heights as the average photon number is increased, is a result of the imperfect visibility V of the interferometer, and the dark counts, whose average number is n_d . The visibility is defined as $V = (\bar{n} - n_b)/(\bar{n} + n_b)$, where n_b is the average number of background counts at $\phi = \pi$. Thus, it can be shown that the peak heights h follow

$$h(\bar{n}) = \exp \left[-\beta \left(n_d + \frac{(1-V)\bar{n}}{2} \right) \right], \quad (5)$$

where $\beta = 2$ for parity and 1 for P_0 . Figure 2 presents the peak height of all measurements with their fits to Eq. 5. The data fits theory very well, where the parity curve

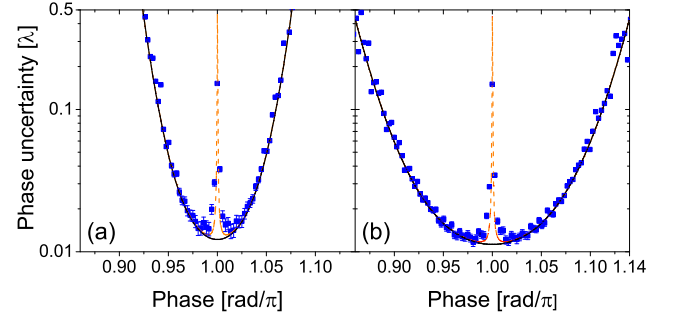


FIG. 3. (color online) Experimental phase uncertainties for 200 photons on average (blue squares), as a function of the phase for (a) parity and (b) P_0 . The theoretical fits to Eqs. 2 and 4 without approximation are presented with solid black lines. Fits to equations that include the effect of imperfect visibility are presented by orange dashed lines. Errors are shown when larger than their symbols. They represent the standard deviation in the phase uncertainty estimation process.

slope is about twice as large as that of P_0 . From the fit parameters of both curves we extract the dark count rate to be 400 ± 100 Hz and the visibility to be 0.99981 ± 10^{-5} , in agreement with independent direct measurements.

The experimental single-shot phase uncertainty for parity and P_0 were calculated from their data using Eqs. 2 and 4, respectively. Representative results for 200 photons on average are presented in Fig. 3. The uncertainty for P_0 is at minimum for a larger range as its peak is also wider. The imperfect visibility is also responsible for the large deviation near $\phi = \pi$ [5]. As the uncertainty in the estimated quantity is a ratio between the uncertainty in the measured quantity and its slope, it can only be finite at this point as long as both contributions approach zero together. Imperfect visibility results in non-zero observed value and non-zero uncertainty in it. Its slope on the other hand is always zero at this point, where this value peaks, resulting in diverging uncertainty in the estimated value. Fits to modified equations which include imperfect visibility due to background counts are also presented, with a good agreement with the results.

A summary of all the results for the range of 2.5 to 4200 photons on average is presented in Fig. 4. The resolutions of parity and P_0 are separated by $\sqrt{2}$ as expected. They are not affected by the imperfect visibility. The phase uncertainty for P_0 is slightly better for small photon numbers, where it follows meticulously the theoretical SNL line. Actually, within experimental errors, the sensitivity of the P_0 measurement is shot-noise limited up to the measurement with 200 photons, where the sensitivity is $\lambda/(86 \pm 2)$ and the resolution is $\lambda/(45 \pm 1)$. Although when more photons are used this limit is not followed anymore, phase sensitivity is further improved, until when using 4200 photons it is $\lambda/(230 \pm 15)$ and the resolution is $\lambda/(202 \pm 2)$. The better sensitivity of P_0 is explained by the dependence on a single measured value,

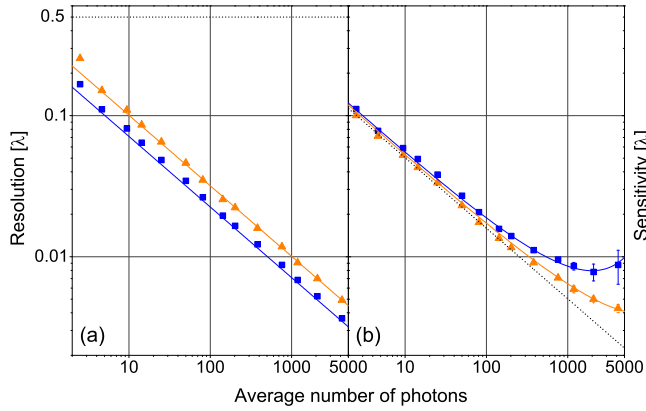


FIG. 4. (color online) (a) The resolution and (b) the smallest uncertainty for parity (blue squares) and P_0 (orange triangles) measurements. Solid lines are the theoretical predictions. For the resolution there are no free parameters and the predictions for sensitivity use the visibility values from the fits of Fig. 2. The parity resolution reaches $\frac{\lambda}{288}$, 144 times better than the Rayleigh $\lambda/2$ limit (dashed line in (a)). The P_0 sensitivity follows the SNL (dashed line in (b)) up to 200 photons. Parity has better resolution but larger deviation from the SNL. Errors were calculated as before and shown when larger than their symbol.

compared to parity that depends on many.

We should emphasize that the values we present here assume photon detection with perfect quantum efficiency. The detector we have used is far from having a perfect efficiency. Nevertheless, this is a frequently used practice, that demonstrates the limit of the method. Moreover, there are other kinds of photon-number resolving detectors with quantum efficiencies that approach unity [26, 27]. Regrettably, they are not available to us.

In conclusion, using a photon-number resolving detector, we have measured the parity and the probability for no-detection of a coherent state that has travelled through a Mach-Zehnder interferometer. Every detected signal is deterministically used for phase evaluation, without post-selection. Super-resolution of these two signals was demonstrated, up to 144 times better than the Rayleigh limit. In addition, these single-shot measurements follow the SNL up to pulses of 200 photons on average, and eventually reach a sensitivity 230 times better than the wavelength. The parity resolution is better than that of P_0 , but the P_0 sensitivity is slightly better and prevails for larger photon numbers. The main limiting factor for these measurements is the visibility of the interferometer.

- [1] G. Meyer and N. M. Amer, Appl. Phys. Lett. **53**, 1045 (1988).
- [2] V. Giovannetti, S. Lloyd, and L. Maccone, Nature Photonics **5**, 222 (2011).
- [3] J. Aasi *et al.*, Nature Photon. **7**, 613 (2013).
- [4] J. P. Dowling, Contemp. Phys. **49**, 125 (2008).
- [5] A. Kuzmich and L. Mandel, Quant. Semiclass. Opt. **10**, 493 (1998).
- [6] M. W. Mitchell, J. S. Lundeen, and A. M. Steinberg, Nature **429**, 161 (2004).
- [7] T. Nagata, R. Okamoto, J. L. O'Brien, K. Sasaki, and S. Takeuchi, Science **316**, 726 (2007).
- [8] I. Afek, O. Ambar, and Y. Silberberg, Science **328**, 879 (2010).
- [9] W. -B. Gao, C. -Y. Lu, X. -C. Yao, P. Xu, O. Gühne, A. Goebel, Y. -A. Chen, C. -Z. Peng, Z. -B. Chen, and J. -W. Pan, Nature Phys. **6**, 331 (2010).
- [10] C. Kothe, G. Björk, and M. Bourennane, Phys. Rev. A **81**, 063836 (2010).
- [11] B. L. Higgins, D. W. Berry, S. D. Bartlett, H. M. Wiseman, and G. J. Pryde, Nature **450**, 393 (2007).
- [12] C. F. Wildfeuer, A. J. Pearlman, J. Chen, J. Fan, A. Migdall and J. P. Dowling, Phys. Rev. A **80**, 043822 (2009).
- [13] G. Khoury, H. S. Eisenberg, E. J. S. Fonseca, and D. Bouwmeester, Phys. Rev. Lett. **96**, 203601 (2006).
- [14] K. J. Resch, K. L. Pagnell, R. Prevedel, A. Gilchrist, G. J. Pryde, J. L. O'Brien, and A. G. White, Phys. Rev. Lett. **98**, 223601 (2007).
- [15] E. Distant, M. Ježek, U. L. Andersen, Phys. Rev. Lett. **111**, 033603 (2013).
- [16] Y. Gao, P. M. Anisimov, C. F. Wildfeuer, J. Luine, H. Lee, and J. P. Dowling, J. Opt. Soc. Am. B **27**, A170 (2010).
- [17] J. J. Bollinger, W. M. Itano, D. J. Wineland, and D. J. Heinzen, Phys. Rev. A **54**, R4649 (1996).
- [18] C. C. Gerry, Phys. Rev. A **61**, 043811 (2000).
- [19] C. C. Gerry and R. A. Campos, Phys. Rev. A **64**, 063814 (2001).
- [20] C. C. Gerry and J. Mimih, Phys. Rev. A **82**, 013831 (2010).
- [21] A. Chiruvelli and H. Lee, J. Mod. Opt. **58**, 945 (2011).
- [22] P. M. Anisimov, G. M. Raterman, A. Chiruvelli, W. N. Plick, S. D. Huver, H. Lee, and J. P. Dowling, Phys. Rev. Lett. **104**, 103602 (2010).
- [23] W. N. Plick, P. M. Anisimov, J. P. Dowling, H. Lee, and G. S. Agarwal, New J. Phys. **12**, 11 (2010).
- [24] L. Dovrat, M. Bakstein, D. Istrati, A. Shaham, and H. S. Eisenberg, Opt. Express **20**, 2266 (2010).
- [25] L. Dovrat, M. Bakstein, D. Istrati, and H. S. Eisenberg, Phys. Scr. **T147**, 014010 (2012).
- [26] E. Waks, K. Inoue, W. D. Oliver, E. Diamanti, and Y. Yamamoto, IEEE J. Sel. Top. Quant. Elect. **9**, 1502 (2003).
- [27] A. E. Lita, A. J. Miller, and S. W. Nam, Opt. Express **16**, 3032 (2008).